ANFIS modeling and Ultrasonic technique for strength and dynamic Elasticity modulus of waste rubber concrete

Abstract

In the present paper, rubberized concrete as a composite material made with different percentages of waste rubber crumbs as a partial replacement of coarse aggregates was investigated by experiment and modeling. For this purpose, different mixtures of rubberized concrete were made by 10% and 15% replacement of waste rubber, while incorporating 10% of the admixtures such as silica fume and zeolite into the binder. rubberized concrete samples were cured at two different relative humidities (RH) of 0.5 and 1, and different tests were carious out at four different ages. Compressive strength and static modulus tests were carried out on different mixtures of cubic and cylindrical samples, respectively. Ultrasonic technique was employed to measure the pulse velocity and dynamic moduli of elasticity of the rubberized concrete samples were determined based compression wave velocity (V_p), shear wave velocity (V_s), and density of the rubberized concrete. The dynamic moduli obtained from ultrasonic were compared to those calculated from ACI-318 equation and the correlation and error were assessed. In order to simulate and predict the compressive strength of the rubberized cement composite in terms of the influencing parameters, namely cement content, silica fume, zeolite, rubber %, RH, and age, ANFIS modeling was implemented and the prediction results and performance criteria were obtained for training, checking, and testing datasets. Parametric study of the ANFIS modeling results was also conducted to investigate each variable's effect on the compressive strength of the rubberized cement composite.

Keywords: waste rubber concrete; Ultrasonic technique; ANFIS modeling; compressive strength; dynamic elasticity modulus

Research Significance

This research was undertaken to address the need of materials recycling through constriction industry and characterization of concrete containing waste rubber and SCMs such as zeolite and silica fume. This is the first time that zeolite has been investigated in rubberized concrete and ANFIS as a machine learning techniques has been used to predict compressive strength of rubberized concrete.

1. Introduction

Among composite material, concrete is the most practical cementitious composite which is known to be the most widely used man-made material in the world, having a variety of types, components and structural and non-structural applications. Hence, its properties are of great importance, as the most widely used composite material throughout the world. Waste materials can be included in concrete and cement composites as their components among which waste tire rubber is an important case [1]. It is estimated that approximately 1.5 billion tire are produced every year and 1 billion tires reach their end of life [2,3]. Consequently, reuse of the waste tires seems to be a promising solution for which the construction industry can be a viable alternative. Due to the concrete high demand, replacing even a small portion of the aggregates by waste rubber crumbs resulted from the waste tires, can be a double advantage of natural resources survival, and waste management. Potential reuses of scrap tire including impact barriers, asphalt or concrete pavements, playground floors, and sports area pavements, have been suggested by various sectors in industry [3,4].

Plain concrete is a composite mainly composed of three parts namely, aggregates (skeleton), cementitious materials (binder), and water. Cement replacement by mineral admixtures and industrial by-products in construction industry has been investigated for several years. It is considered as a Multi-faceted benefit comprising energy/ environment saving through cement/ CO_2 footprint reduction plus waste management, cost-effectiveness, as well as strength and durability enhancement of the concrete. The supplementary cementitious materials include nanomaterials [5-7], fly ash [8], silica fume [9], slag [10] and some other types of admixtures that can help reduce the cement content while enhancing the durability, and thereby leading to a more sustainable composite structures.

With regard to mechanical properties of rubberized concrete, the main advantages obtained include energy absorption, enhanced ductility, and damping capacity [11-15]. These are of great importance when energy absorption is preferred over the strength. Nonetheless, reduced strength

and stiffness and as a result lower durability performance, namely lower resistance to carbonation and chloride attack are the weaknesses reported in rubberized concrete studies [16].

Replacement of the aggregates by rubber crumbs weakens the concrete skeleton, while addition of the pozzolanic admixtures helps strengthen the paste. As a results, application of both will results in a trade-off in which the latter partially compensates for the mechanical and durability loss due to the former. This makes the behavior prediction of the composite structure even more complicated which is why most of the available studies and assessments are essentially experimental works [14-19]. However, in order to capture and predict the overall behavior of this composite based on its ingredients, computer-aided tools are extremely valuable to model the composite materials. Several computer-aided prediction models, namely multiple regressions (MR), artificial neural network (ANN), fuzzy logic (FL), genetic programming (GP), etc. have been utilized by researchers to predict the properties of composite structure [20-22] and materials [23-25]. Amongst the aforementioned methods, adaptive neuro-fuzzy inference system (ANFIS) utilizes the capability of neural networks (NNs) and fuzzy logic (FL) to well capture the behavior which results in a an easier and more robust modeling and prediction results. Nondestructive testing such as ultrasonic technique has also been used by researcher as a useful tool to estimate the mechanical properties of concrete.

In the present study, an experimental program was conducted to assess the compressive strength and dynamic elasticity of the concrete containing scrap tires to partially replace the concrete skeleton (aggregates), as well as silica fume (SF) and zeolite (ZE) to replace a fraction of the paste (binder). Different mixtures were made and a series of tests were carried out to measure the density, compressive strength, and elastic modulus. Ultrasonic test as a nondestructive tool was also conducted to measure the secondary pulse velocity in order to estimate the dynamic elasticity modulus of the rubberized concrete. Based on the composite ingredients, ANFIS model was developed to predict the compressive strength of the waste rubber concrete as a function of binder ingredients (cement, SF, ZE), rubber percentage, relative humidity (RH) for curing condition, and age. Parametric study was also conducted to assess the interactions of the variables on compressive strength of the rubberized concrete.

2. Experimental program

In order to make the rubberized concrete mixtures, the coarse aggregates were partially replaced by 10% and 15% of waste rubber crumbs. The rubber crumbs were graded so as to have a similar gradation to the coarse aggregates. Cement was replace by silica fume (SF) and zeolite (ZE) by 10% in some concrete mixes to investigate the effect of the admixtures on the binder in particular and on rubberized concrete in general. Table 1 shows the composition of the powder materials used in this study. Cement type II was used in this study and binder content was considered as 400 Kg/m^3.

Table 1. Chemical composition of silica fume ad cement

Composition	**Cement**	**Silica fume**	**Zeolite**
SiO2	21.37	93.16	66.5
Al2O3	4.83	1.13	11.81
Fe2O3	3.34	0.72	1.3
CaO	62.46	-	3.11
MgO	3.62	1.6	0.72
SO3	1.76	0.05	0.26
Na2O	0.18	-	2.01
K2O	0.51	-	3.12
L.O.I	1.87	1.58	12.05

The abbreviation used for the mixture designation, RB, C, SF, ZE, and D represents rubber, control, silica fume, zeolite, and dry curing, respectively. For instance, 10RB.ZE.D means the concrete mixture containing 10% of rubber and 10% of zeolite with dry curing. According to ACI 211-91, the ratio of gravel to sand was selected as 60% to 40%. In order to investigate the effect of curing on mechanical properties of the rubberized concrete, two different curing conditions as wet and dry were used with relative humidity (RH) of 100% and 50%, respectively.

In order to test the compressive strength, cubic samples of 150*150*150 mm dimensions were made according to ASTM C39, and three replica were tested for each mix.

The static elasticity modulus of the rubberized concrete was measured conforming to ASTM C469 which was carried out on cylindrical samples of 150*300 mm dimensions. In this procedure, the sample is fixed between two yokes with distance of 150mm from each other. During load application, the applied load and axial strain were recorded in two steps:

a) When strain value of 0.000050 was reached ($\varepsilon_1 = 50 * 10^{-6}$)
b) Once 40% of ultimate load is reached (ε_2)

Then the static elasticity modulus can be calculated by Eq. (1):

$$E = (S_2 - S_1)/(\varepsilon_2 - 50 * 10^{-6}) \quad (1)$$

E= chord modulus of elasticity

S2=stress corresponding to 40% of the ultimate load of the concrete

S1=stress corresponding to a longitudinal strain of ε1 at 50 millionths

ε2=longitudinal strain produced by S2

3. Ultrasonic pulse velocity and dynamic elasticity modulus

One of the important properties which can be estimated through ultrasonic technique is elasticity modulus which can be used for design purpose. According to ASTM C597, the relationship between pulse velocity and elasticity modulus can be described by Eq. (2):

$$V = \sqrt{\frac{E(1-\nu)}{\rho(1+\nu)(1-2\nu)}} \quad (2)$$

Where,

E: dynamic modulus of elasticity (kN/mm^2)

ν: Poisson's ratio

ρ: concrete density (kg/m^3)

For calculation of elasticity modulus, first Poisson's ratio needs to be calculated through the following equation:

$$v = \frac{V_p^2 - 2V_s^2}{2(V_p^2 - V_s^2)} \quad (3)$$

Where V_p and V_s are compression and shear wave velocity in km/sec respectively.

Then, shear modulus (G) is calculated by the equation presented below:

$$G = \rho V_s^2 \quad (4)$$

Finally, the modulus of elasticity can be calculated by Eq. (5):

$$E = 2G(1 + v) \quad (5)$$

4. Determination of ultrasonic secondary waves

Secondary or shear waves denoted by V_S are a type of seismic waves which are required for determination of dynamic modulus of elasticity of concrete using ultrasonic apparatus. There are two types of transducers generating primary (compression) and secondary (shear) waves. In order to measure the secondary waves, the suitable transducers generating secondary waves need to be installed on the sample.

The apparatus used was PUNDIT6 as illustrated in Fig. 1. In this machine repetitive voltage pulses are generated electronically and transformed into wave bursts of mechanical energy by the transmitting transducer, which must be coupled to the concrete surface through a suitable medium.

Fig. 1. PUNDIT device to measure the ultrasonic pulse velocity in concrete samples

A similar receiving transducer is also coupled to the concrete at a known distance from the transmitter, and the mechanical energy converted back to electrical pulses of the same frequency. The electronic timing device measures the interval between the onset and reception of the pulse and this is displayed either on an oscilloscope or as a digital readout.

Since the maximum pulse energy is transmitted in arrangement called Opposite faces (direct transmission), it was taken as transducers arrangement as shown in Fig. 2.

Fig. 2. Direct method to measure the pulse velocity in concrete samples

5. ANFIS modeling

ANFIS is the famous hybrid neuro-fuzzy network for modeling the complex systems [26, 27]. ANFIS incorporates the human-like reasoning style of fuzzy systems through the use of fuzzy sets and a linguistic model consisting of a set of If-Then fuzzy rules. The main strength of ANFIS models is that they are universal approximators [26] with the ability to solicit interpretable If-Then rules.

The architecture of an ANFIS model with two input variables is shown in Fig. 3 assuming two IF-THEN rules for fuzzy mechanism of Sugeno type, we will have the following for the ANFIS reasoning:

Rule 1: IF x is A_1 and y is B_1, THEN $f_1=p_1x+q_1y+r_1$

Rule 2: IF x is A_2 and y is B_2, THEN $f_2=p_2x+q_2y+r_2$

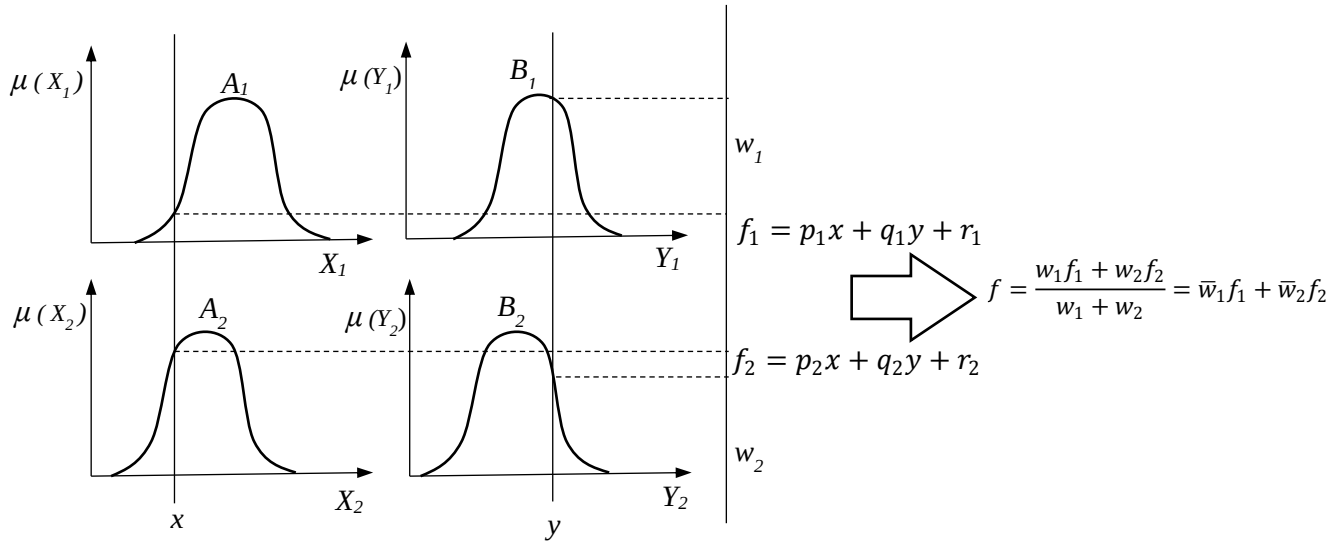

Fig. 3. The reasoning scheme of ANFIS

The ANFIS architecture corresponding to the reasoning system provided in Fig. 4, is illustrated in Fig. for which each layer can be described as follows:

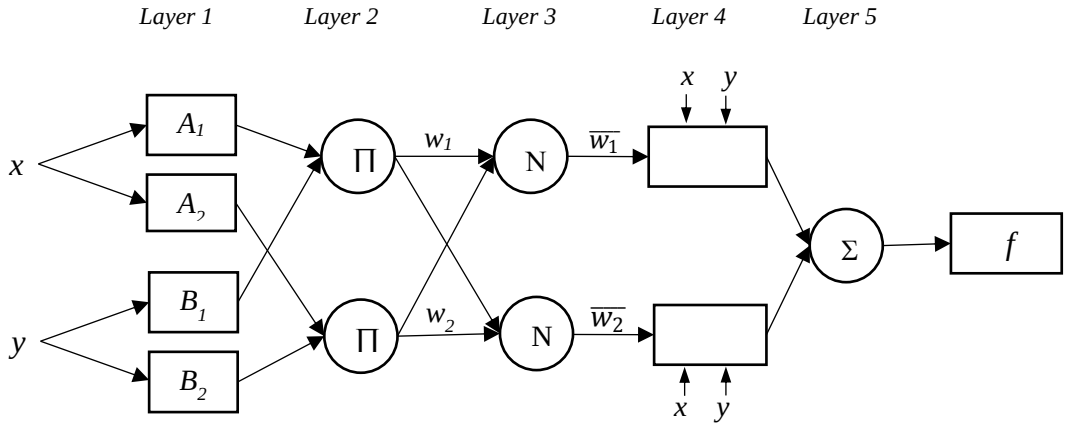

Fig. 4. Schematic of ANFIS architecture

Layer 1) Every node *i* in this layer is a square node with a node function:

$$Q_i^1 = \mu_{A_i}(x) \tag{6}$$

where *x* is the input to node *i*, and A_i is the linguistic label (fuzzy sets: small, large, …) associated with this node function. Premise parameters change the shape of the membership function.

Layer 2) Every node in this layer is a circle node labeled ∏ which multiplies the incoming signals and sends the product out. For instance ∏-norm operation:

$$Q_i^2 = \mu_{A_i}(x) \times \mu_{B_i}(y), i = 1, 2 \quad (7)$$

Layer 3) Every node in this layer is a circle node labeled *N*, representing the normalized firing strength of each rule. The i^{th} node calculated the ratio of the i^{th} rule's firing weight to the sum of all rule's firing weights. The outputs of this layer are called normalized firing strengths.

$$Q_i^3 = \overline{w}_i = \frac{w_i}{w_1 + w_2}, i = 1, 2 \quad (8)$$

Layer 4) Every node in this layer is an adaptive node with a node function, indicating the contribution of the i^{th} rule towards the overall output.

$$Q_i^4 = \overline{w}_i f_i = \overline{w}_i (p_i x + q_i y + r_i), i = 1, 2 \quad (9)$$

where $\overline{w}_i$ is the output of layer 3, and {*pi*, *qi*, *ri*} is the parameter set.

Layer 5) The signal node in this layer is a circle node labeled ∑, indicating the overall output as the summation of all incoming signals calculated, i.e.

$$Q_i^5 = \sum_i \overline{w}_i f_i = \frac{\sum_i w_i f_i}{\sum_i w_i} \quad (10)$$

ANFIS include a rapid learning method named as hybrid-learning method which utilizes the gradient descent and the least-squares method to find a feasible set of antecedent and consequent parameters [27, 28]. Thus in this paper, the later method was used to build the prediction model.

5.1.ANFIS model structure and parameters

The structure of the ANFIS model included six variables namely, cement content (C), silica fume content (SF), zeolite content (ZE), rubber percentage (RB), relative humidity of curing condition (RH), and the age of the samples (Age), and one output, i.e. compressive strength of rubberized concrete (fc). From the total 72 experimental datasets, training, checking, and testing datasets were randomly selected as 52, 10, 10 datasets, respectively. Two different models were constructed based on two series of randomly selected data in order to investigate the effect of data selection on ANFIS modeling results.

MATLAB R2017 toolbox was used in this study. There are two methods to construct the model in MATLAB ANFIS toolbox, namely grid partition and subtractive clustering. With the number of inputs growing in the grid partition model, the membership function shows exponential growth, and thereby leading to a paralyzed calculation system. By using the subtractive clustering method,

it is easy to generate an input–output rule model without being computationally expensive [29-31].

6. Results and discussion

6.1. Ultrasonic secondary wave velocity results

The results of secondary wave velocities are reported in Fig. 5. The measurements were implemented at various ages as 3, 7, 28 and 42 days. In order to compare the curing conditions effect on the secondary wave velocity in rubberized concrete samples, the results are shown in plots (a) and (b) for RH=1 and RH=0.5, respectively.

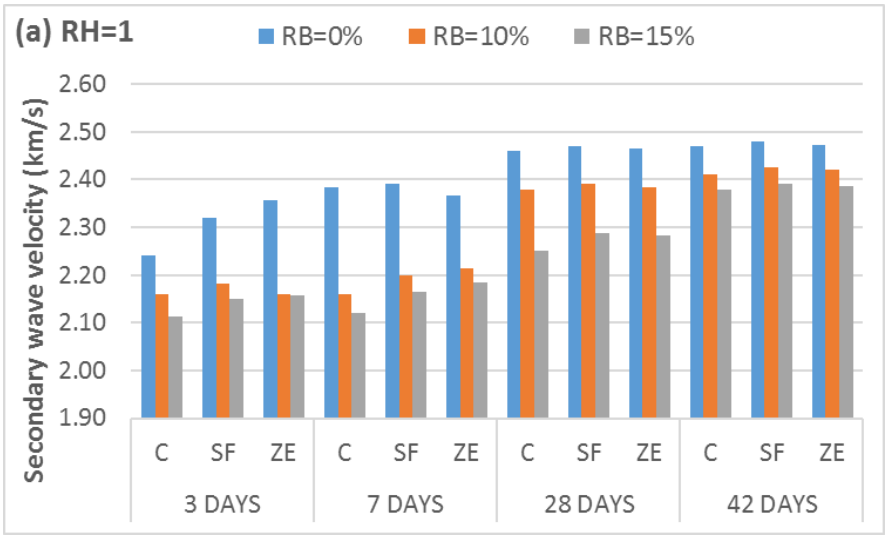

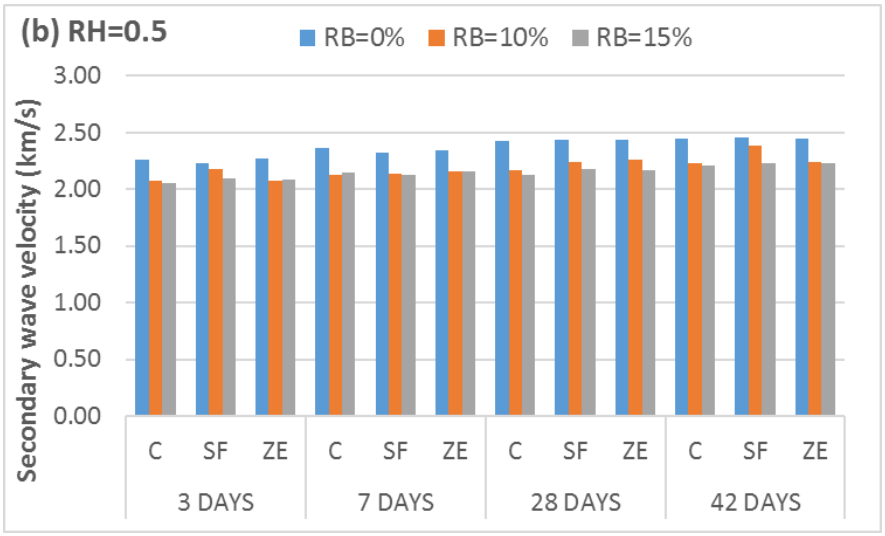

Fig. 5. Secondary pulse velocity in rubberized concrete (a) for RH=1, and (b) for RH=0.5

The results apparently show that the secondary wave velocities increased by age of the concrete. As can be noted from the table, even though there are some discrepancies among the results, but in most of the cases the velocity decreased in dry condition compared to wet curing. Another factor obviously affecting the pulse velocity is rubber addition to the concrete which reduces the stiffness and thereby leading to wave velocity decrease.

6.2.Static modulus results

Based on the tests carried out on rubberized concrete cylinders with dimensions of 150*300 mm according to ASTM C469 by using the Eq. (1), the static elasticity modulus was calculated as reported in Table 2. The measurements were implemented at four different ages namely, 3, 7, 28, and 42 days in order to assess the effect of age on elastic modulus of the rubberized concrete.

Table 2. static elasticity modulus results obtained from the tests on cylindrical samples of rubberized concrete

Static Elasticity Modulus				
Sample ID	3 days	7 days	28 days	42 days
0RB.C	18.236	24.434	28	28.456
0RB.C.D	19.33	21.51	26.34	27.066
0RB.SF	19.941	24.668	28.67	29.03
0RB.SF.D	18.427	20.11	24.89	27.546
0RB.ZE	21.166	24.58	28.28	28.638
0RB.ZE.D	19.61	21.712	26.67	27.402
10RB.C	14.52	16.896	24.316	25.492
10RB.C.D	13.192	13.838	16.47	18.369
10RB.SF	15.338	18.033	24.5	26.024
10RB.SF.D	14.472	15.33	18.63	24.032
10RB.ZE	16.483	18.55	24.368	25.774
10RB.ZE.D	14.586	15.77	19	18.593
15RB.C	13.16	15.721	18.865	24.008
15RB.C.D	12.514	13.991	15.44	17.71
15RB.SF	14.224	16.051	18.895	24.48

15RB.SF.D	13.444	14.865	16.88	18.01
15RB.ZE	14.52	16.717	20.3	24.314
15RB.ZE.D	13.397	14.338	16.55	18.093

6.3.Dynamic modulus of elasticity from ultrasonic

Based on the relationship presented earlier, dynamic modulus of elasticity of concrete can be calculated. As mentioned earlier, the parameters needed in order to calculate the dynamic modulus of elasticity include poison's ratio (ν) which is calculated from compression (V_p) and shear wave velocity (V_s), as well as the density of the concrete samples (ρ). Listed in Table 3 are the results of dynamic modulus of elasticity obtained from ultrasonic waves at various ages.

Table 3. Dynamic elasticity modulus results obtained from ultrasonic technique

Dynamic Elasticity Modulus (GPa)				
Sample ID	3 days	7 days	28 days	42 days
0RB.C	28.399	34.747	36.850	37.248
0RB.C.D	30.664	32.408	35.470	36.057
0RB.SF	31.153	34.934	37.430	37.740
0RB.SF.D	29.942	31.288	35.910	36.468
0RB.ZE	32.133	34.064	37.090	37.404
0RB.ZE.D	30.890	31.785	35.740	36.344
10RB.C	26.820	27.896	33.850	34.794
10RB.C.D	25.754	24.838	27.470	29.277
10RB.SF	27.470	29.025	34.000	35.219
10RB.SF.D	26.778	26.330	29.470	33.626
10RB.ZE	28.386	29.413	33.894	35.019
10RB.ZE.D	26.869	26.770	30.000	29.445
15RB.C	25.730	26.721	29.870	33.606
15RB.C.D	25.211	26.393	26.440	28.710
15RB.SF	26.579	28.041	30.895	33.984
15RB.SF.D	25.955	25.087	27.880	29.008
15RB.ZE	26.816	28.574	30.725	33.851
15RB.ZE.D	25.918	26.670	27.550	29.070

For the purpose of clarity, the results of dynamic moduli are depicted in Fig. 6 (a) and (B) for different RHs at different ages. It can be said that the results are directly proportional to ultrasonic pulse velocity, i.e. higher wave velocity results in higher dynamic modulus of elasticity. It can be

found from the figure that rubber addition reduces the dynamic modulus, however ZE and SF addition can increase the dynamic modulus in concrete samples. According to the results, replacement of coarse aggregates with waste rubber crumbs by 10% and 15% has roughly led to 7% and 15% reduction in dynamic modulus, respectively, in the curing condition with RH=1. Nevertheless, it is seen from the plots that the dynamic modulus increase in rubberized concrete samples by age in RH=0.5 is not as significant.

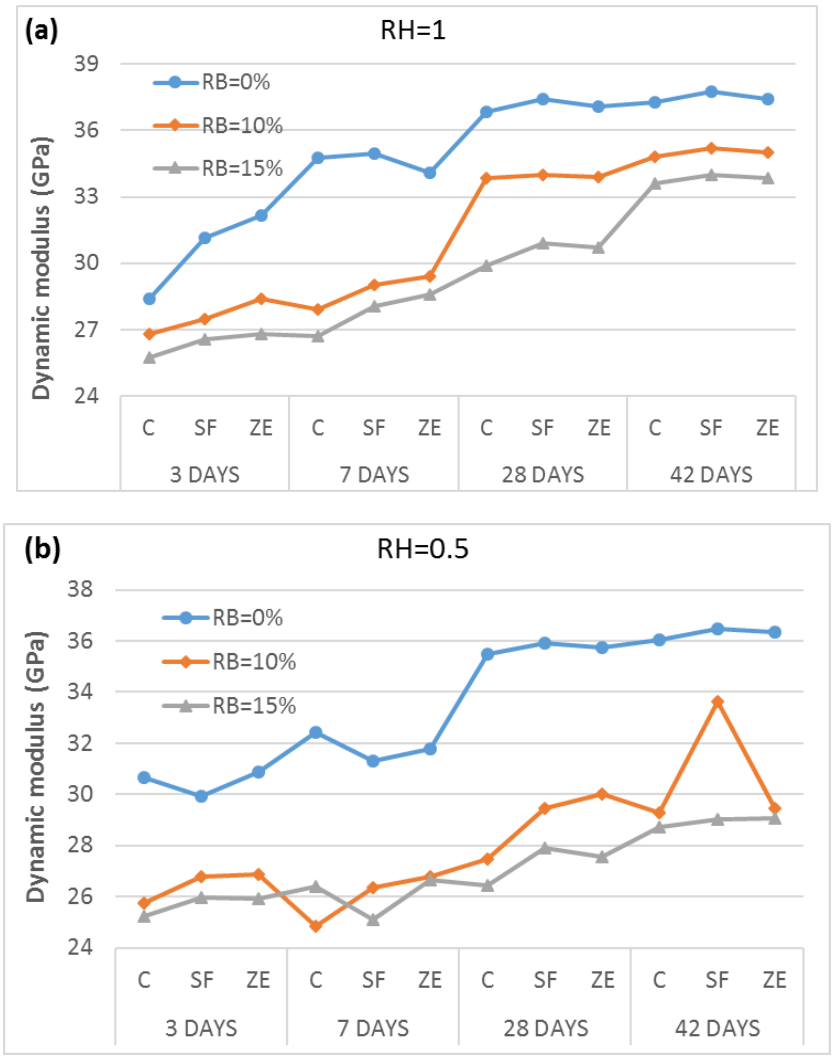

Fig. 6. Comparative plots of dynamic modulus at different RB%, age, and RH

6.4.Comparison of dynamic modulus with ACI standard

In order to validate the dynamic moduli obtained from ultrasonic technique, they can be compared with the dynamic moduli obtained from static moduli based on the relationship given in ACI standard. The relationship between static and dynamic elasticity moduli according to ACI318-83 is as following:

$$E_s = (1.25 * E_d) - 19 \quad (11)$$

which can be rearranged as:

$$E_d = 0.8 \times (E_s + 19) \quad (12)$$

where E_s is the static modulus obtained from the experiment and E_d is the dynamic modulus. In order for comparison, the results of dynamic moduli obtained from ultrasonic and standard equations are plotted in Fig. 7 for different relative humidities at 42 days of age.

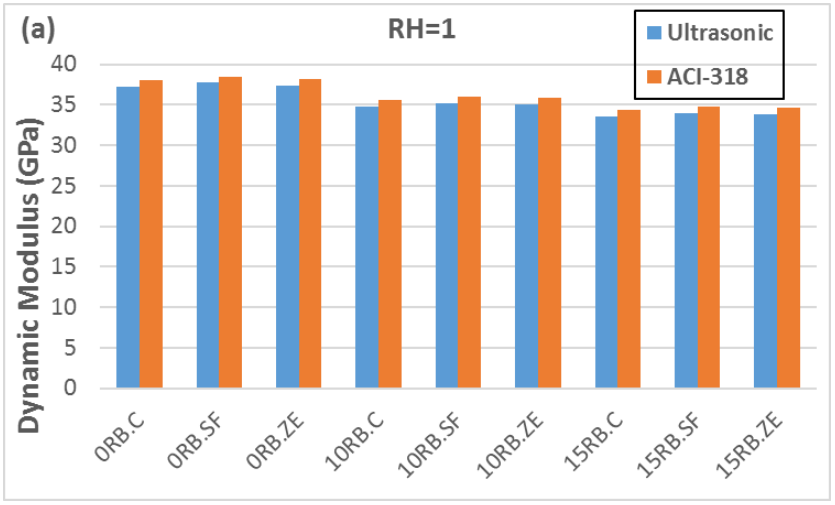

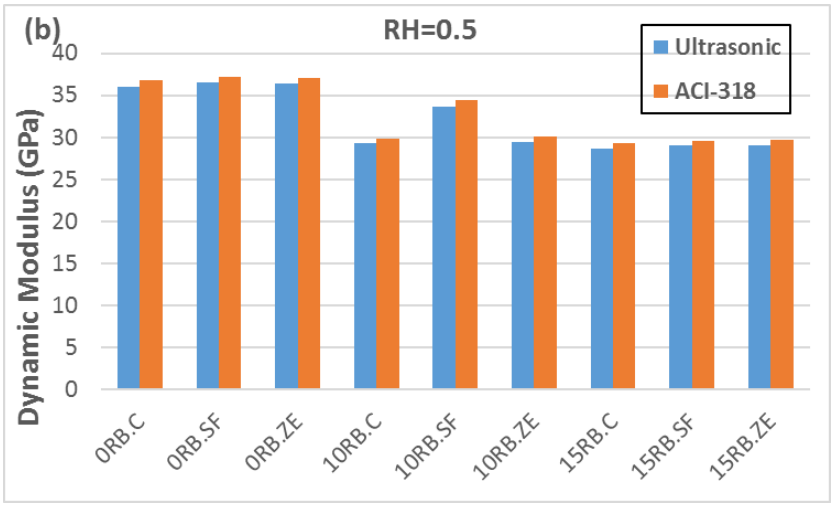

Fig. 7. Comparison of dynamic modulus obtained from ultrasonic and ACI-318 equation

As ca be seen from the plots, the results obtained from ultrasonic are in a very good agreement with the ACI standard equation. By comparing Fig. 7(a) and (b), it is also noted that the dynamic modulus drop due to rubber addition is greater for curing condition with RH=0.5. It can also be seen that the addition of SF and ZE has slightly strengthen the binder of rubberized concrete, and thereby leading to small increase of dynamic modulus.

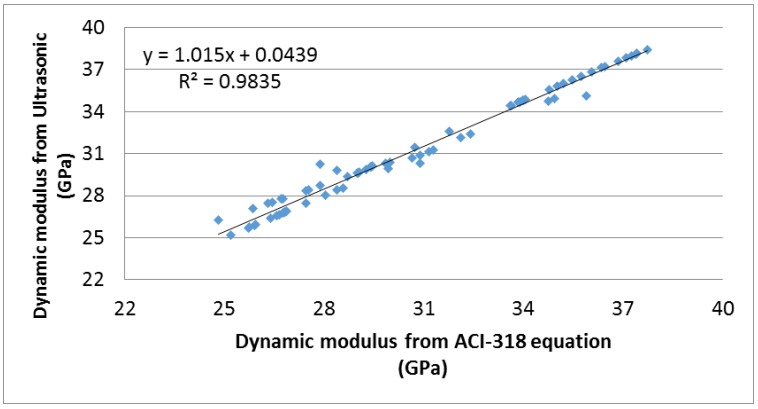

(a)

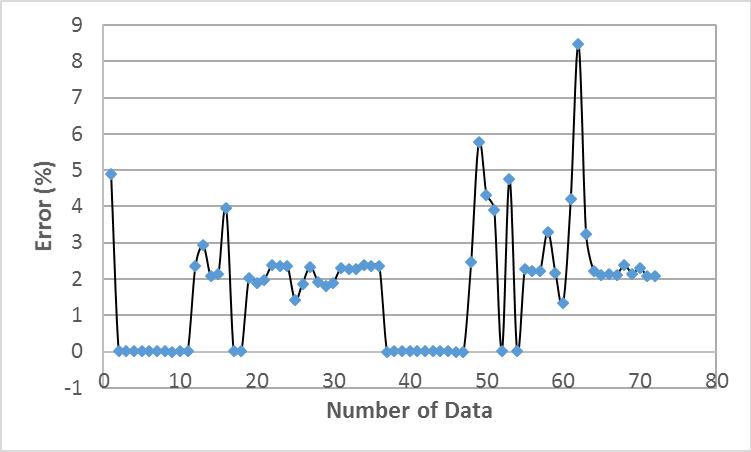

(b)

Fig. 8. (a) Correlation and (b) error of dynamic elasticity moduli obtained from ultrasonic vs. ACI equation:

For better comparison, the correlation between the dynamic modulus values resulted from ultrasonic and ACI equation, along with the error (difference) are plotted in Fig 8 (a) and (b) respectively. The measured data points are 72 that include all the measurements at different ages and curing conditions. As is seen, the correlation between results is pretty high and errors are very small with average of 1.76 %.

6.5.Compressive strength results

The strength results of rubberized concrete samples at different ages in various curing conditions are presented in table 4. As mentioned before, two curing conditions were considered as wet and dry. For wet conditions, the samples were submerged in the water tank and for dry curing, they were kept in a covered room with relative humidity of 50%. As can is noted from the results in the table, strengths of the samples cured in dry condition are all lower than those of wet-cured condition. This is apparently due to availability of more humidity in wet condition for better hydration of the cementitious materials. It can be seen form the table that typically the strength trends increase from control sample to the samples containing ZE, and again go higher for the samples incorporating SF in both curing conditions. Even though the increase is small, however it is confirmed that 10% addition of these pozzolans can enhance the strength of the rubberized concrete in wet and dry curing conditions.

Table 4. Compressive strength results of rubberized concrete for different curing conditions at various ages

Wet cured												
	3 days			**7 days**			**28 days**			**42 days**		
(MPa)	0RB	10RB	15RB	0RB	10RB	15RB	0RB	10RB	15RB	0RB	10RB	15RB
C	14.6	8.44	6.41	22.17	11.96	9.91	40.01	21.58	16.91	42.28	27.46	20.04
SF	14.62	9.33	7.49	23.34	13.16	10.2	43.33	22.49	18.31	45.15	30.12	22.4
ZE	14.84	8.7	7.36	22.9	12.16	10.13	41.4	21.84	17.52	43.19	28.87	21.57
Dry cured												
	3 days			**7 days**			**28 days**			**42 days**		
(MPa)	0RB	10RB	15RB	0RB	10RB	15RB	0RB	10RB	15RB	0RB	10RB	15RB
C	11.92	6.6	5.37	16.56	7.98	7.58	31.68	14.08	11.08	35.33	18.71	17.21
SF	12.57	8.07	6.48	16.63	10	9.02	34.45	18.31	14	37.73	20.16	18.47
ZE	12.18	7.19	5.75	16.8	9.27	7.78	33.35	17.39	12.94	37.05	18.96	17.8

In order for a better comparison of the strength trends, the compressive strength results are plotted in Fig. 9. As can be seen from the figure, addition of 10% rubber causes a sudden drop in the concrete strength which continues to drop by rubber addition to 15% to a lesser extent. Quite similar trends are observed for both curing conditions, with a difference that at the age of 42 days, trends of the mixtures containing 10% and 15% rubber crumbs cured at RH=0.5 are closer that those cured in RH=1.

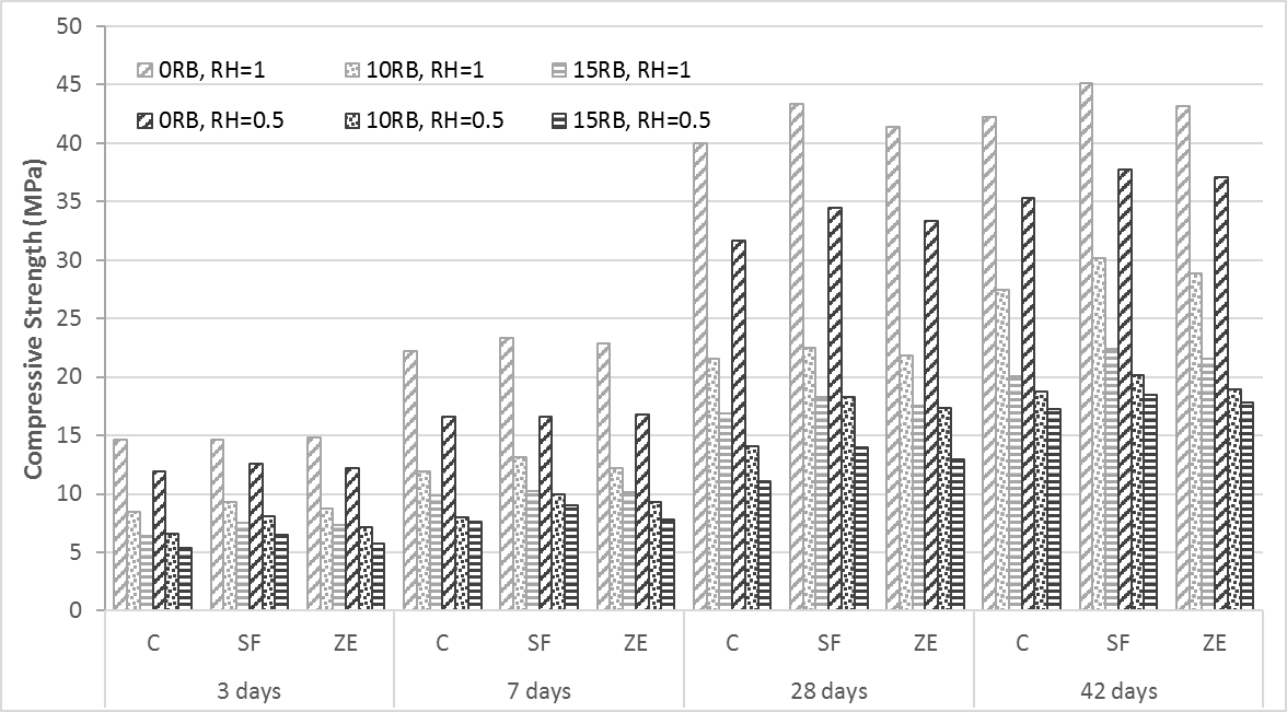

Fig. 9. Comparison of strength results of rubberized concrete for different mixtures

In order to scrutinize the effect of waste rubber replacement on compressive strength of the rubberized concrete, results of strength loss of the rubber-contained samples compared to the non-rubberized samples are plotted in Fig. 10. It can be vividly seen that the strength loss has decreased at later ages. It is also noteworthy that the addition of SF and ZE has resulted in a less strength loss. It is also worth noticing the combinatory effect of variables such as RH and age; at early ages the drop for RH=1 is equal or more than that of RH=0.5, however at later ages especially at 42 days, the strength drops for the samples cured at RH=1 have notably decreased.

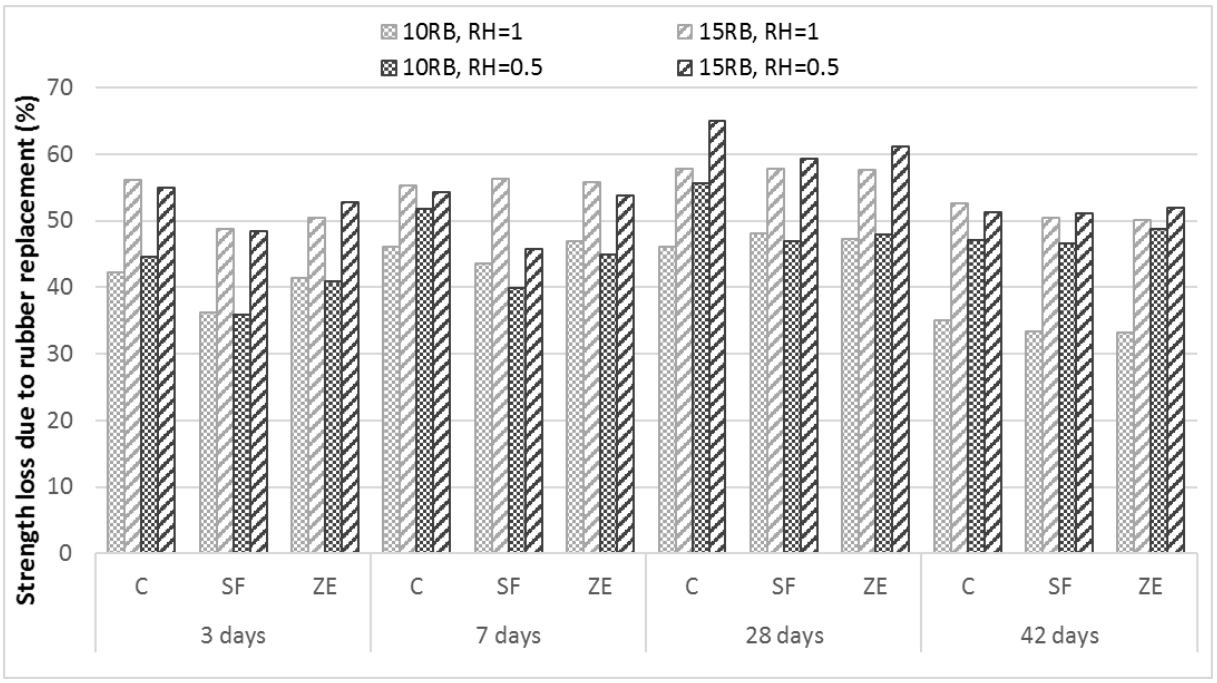

Fig. 10. Percentage of compressive strength loss due to rubber replacement

6.6.ANFIS modeling results

The architecture of the ANFIS model including six inputs and one output with Sugeno-type inference system is displayed in Fig. 11. As mentioned earlier, subtractive clustering method was used to build the ANFIS model which is quite faster and more optimized in assigning the membership functions (MFs) and generating the rules, and thereby resulting in more accurate and less computationally expensive model.

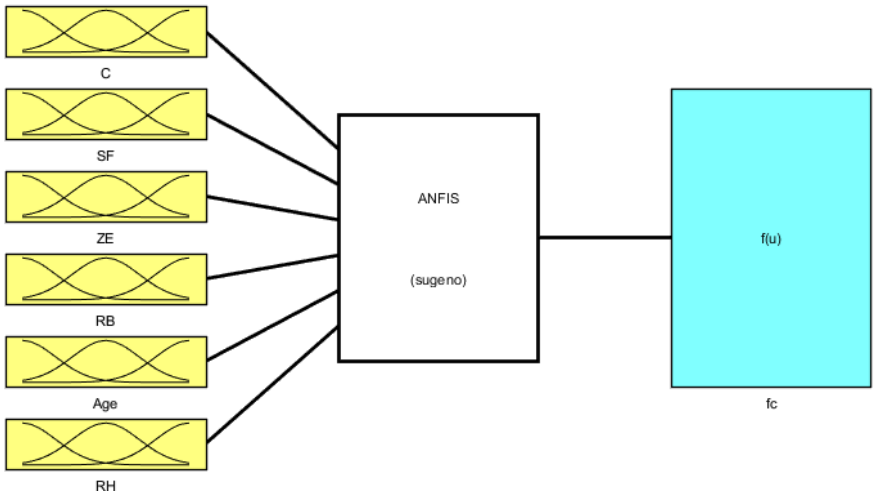

Fig. 11. Architecture of ANFIS model with six inputs and one output

The ANFIS five-layer structure of inputs, input membership functions (inpuMFs), Rules, output membership functions (outputMFs), and outputs as constructed in MATLAB are graphically illustrated in Fig. 12.

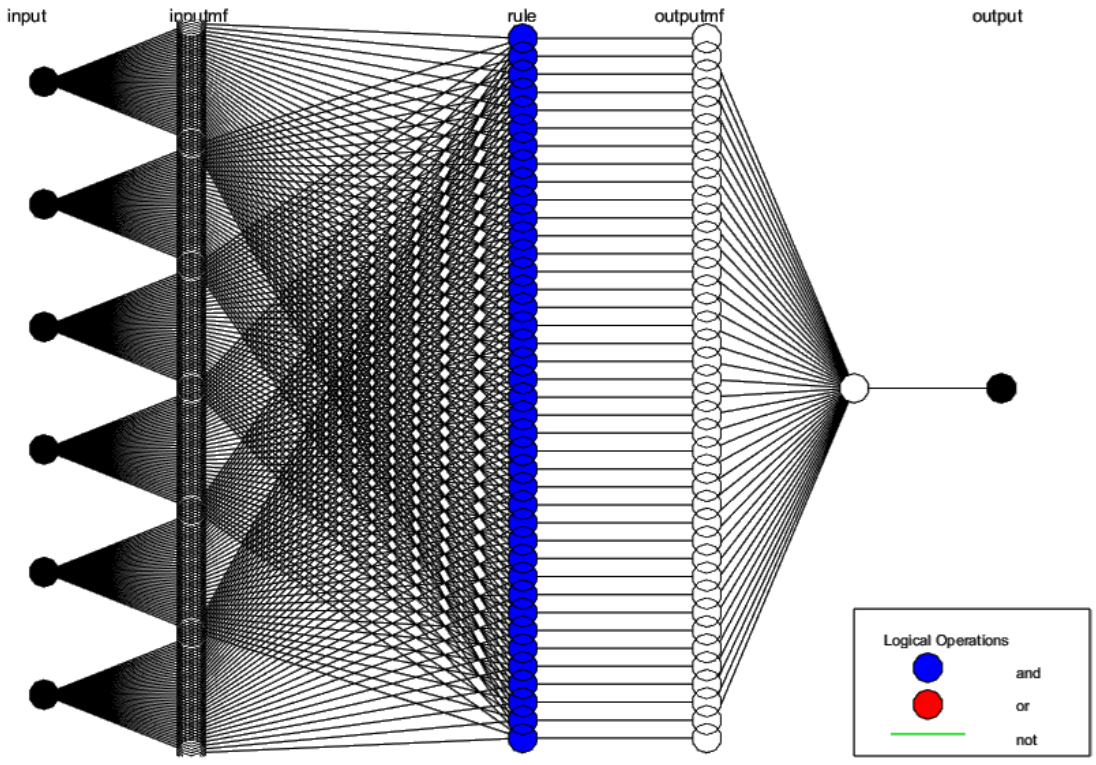

Fig. 12. the structure of the ANFIS model with the generated rules

In this study, absolute fraction of variance ($R2$) was employed to describe the correlation factor which is calculated by Eq. (13) [31]. Two other criteria as mean absolute percent error (MAPE) and root mean square error (RMSE) were also considered to calculate the error involved in training, checking, testing, and all data.

$$R^2 = 1 - \left(\frac{\sum_i (t_i - o_i)^2}{\sum_i (o_i)^2}\right) \quad (13)$$

$$MAPE = \frac{1}{n}\sum_i \left|\frac{t_i - o_i}{t_i}\right| \times 100 \quad (14)$$

$$RMSE = \sqrt{\frac{1}{n}\sum_i (t_i - O_i)^2} \quad (15)$$

All of the results obtained from experimental studies and predicted by ANFIS for the training, checking and testing are given in Fig. 13a, b and c, respectively. The linear least square fit line, its equation and the R^2 values have been shown in these figures. Besides, inputs values and experimental results along with checking and testing results obtained from ANFIS-I and ANFIS-II models are given in Table 5. As it is visible in Fig. 13, the values obtained from the training, validating and testing in ANFIS-I and ANFIS-II models are in a good agreement with the experimental results. The result of testing phase in Fig. 13c indicates that the ANFIS-I and ANFIS-II models are capable of generalizing between input and output variables with reasonably good predictions. In order to assess and compare the performance of the ANFIS models, the values of the performance criteria, namely R^2, MAPE, and RMSE for training, checking, testing, and all datasets for ANFIS-I and ANFIS-II are reported in table 6. Based on the performance criteria, it is observed that R^2 values of training datasets are pretty high and equal for both ANFIS-I and ANFIS-II. However, checking results show a little lower R^2 and the corresponding value for testing results is lower which proves the correct performance of the ANFIS models. The results obtained especially from testing datasets indicate that ANFIS-II model is superior that ANFIS-I. Nevertheless, it is noted that all R^2 values are quite high, proving the fact that the proposed ANFIS models are pretty robust in predicting the complicated behavior of the rubberized cement composites by taking into account various influencing parameters.

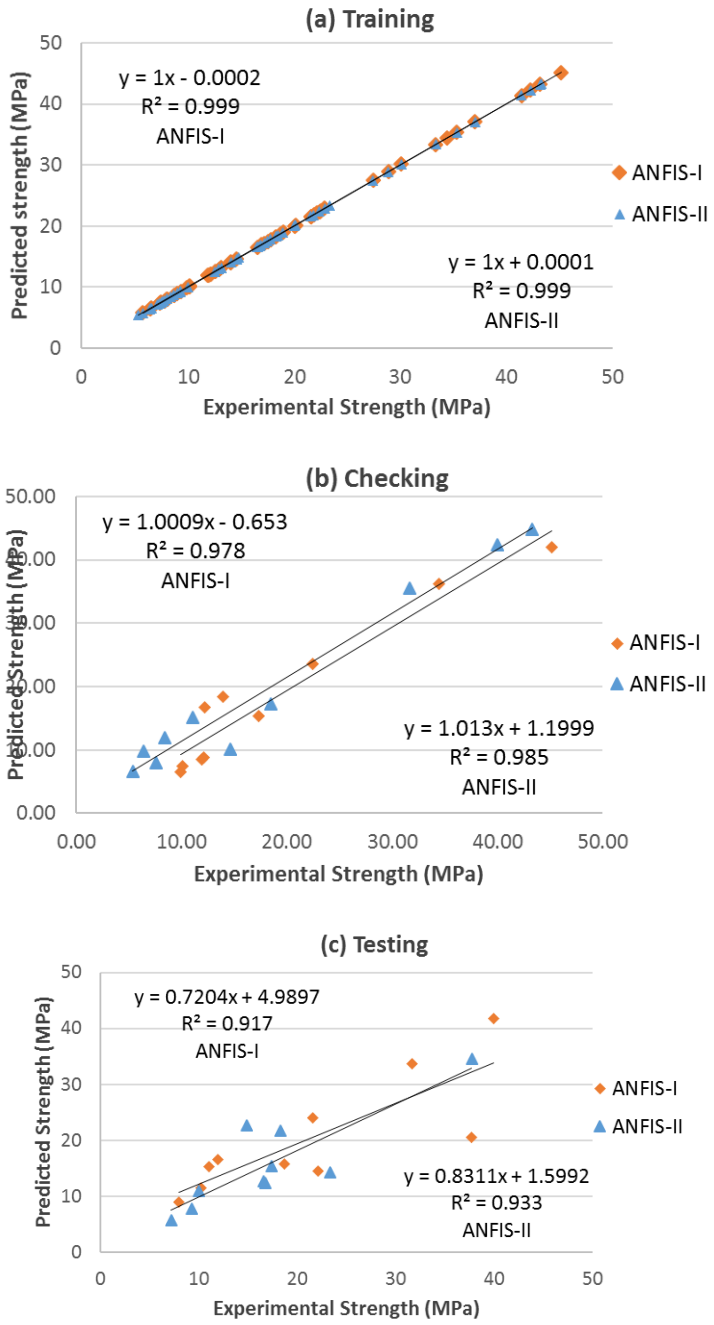

Fig. 13. correlation of the measured and predicted compressive strength values of rubberized concrete for (a) training and (b) validating and (c) testing phase of ANFIS models.

Table 5. Data sets for comparison of experimental results with checking and testing results predicted from ANFIS-I and ANFIS-II models

	ANFIS-I

Phase	C	SF	ZE	RB	Age	RH	Experimental fc	Predicted fc
Checking	360.00	0.00	40.00	10.00	28.00	0.50	17.39	15.40
	360.00	0.00	40.00	15.00	7.00	1.00	10.13	7.46
	360.00	40.00	0.00	0.00	28.00	0.50	34.45	36.24
	400.00	0.00	0.00	15.00	7.00	1.00	9.91	6.49
	360.00	40.00	0.00	15.00	28.00	0.50	14.00	18.34
	360.00	40.00	0.00	10.00	28.00	1.00	22.49	23.62
	400.00	0.00	0.00	10.00	7.00	1.00	11.96	8.45
	360.00	0.00	40.00	10.00	7.00	1.00	12.16	8.83
	360.00	0.00	40.00	0.00	3.00	0.50	12.18	16.66
	360.00	40.00	0.00	0.00	42.00	1.00	45.15	41.96
Testing	400.00	0.00	0.00	0.00	28.00	0.50	31.68	33.77
	400.00	0.00	0.00	0.00	28.00	1.00	40.01	41.83
	360.00	0.00	40.00	15.00	42.00	1.00	21.57	24.10
	400.00	0.00	0.00	10.00	7.00	0.50	7.98	9.09
	400.00	0.00	0.00	15.00	28.00	0.50	11.08	15.41
	360.00	40.00	0.00	0.00	42.00	0.50	37.73	20.54
	400.00	0.00	0.00	0.00	3.00	0.50	11.92	16.56
	400.00	0.00	0.00	0.00	7.00	1.00	22.17	14.60
	400.00	0.00	0.00	10.00	42.00	0.50	18.71	15.86
	360.00	40.00	0.00	15.00	7.00	1.00	10.20	11.62
ANFIS-II								
Checking	400.00	0.00	0.00	15.00	7.00	0.50	7.58	7.97
	360.00	40.00	0.00	0.00	3.00	1.00	14.62	10.07
	400.00	0.00	0.00	0.00	28.00	1.00	40.01	42.34
	400.00	0.00	0.00	10.00	3.00	1.00	8.44	11.93
	400.00	0.00	0.00	15.00	3.00	1.00	6.41	9.86
	400.00	0.00	0.00	0.00	28.00	0.50	31.68	35.47
	400.00	0.00	0.00	15.00	3.00	0.50	5.37	6.60
	360.00	40.00	0.00	0.00	28.00	1.00	43.33	44.80
	400.00	0.00	0.00	15.00	28.00	0.50	11.08	15.14
	360.00	40.00	0.00	15.00	42.00	0.50	18.47	17.23
Testing	360.00	0.00	40.00	0.00	7.00	0.50	16.80	12.39
	360.00	0.00	40.00	0.00	3.00	1.00	14.84	22.74
	360.00	0.00	40.00	10.00	28.00	0.50	17.39	15.38
	360.00	40.00	0.00	0.00	42.00	0.50	37.73	34.49
	360.00	40.00	0.00	0.00	7.00	0.50	16.63	12.79
	360.00	0.00	40.00	10.00	7.00	0.50	9.27	7.80
	360.00	40.00	0.00	10.00	7.00	0.50	10.00	11.02
	360.00	40.00	0.00	15.00	28.00	1.00	18.31	21.79
	360.00	0.00	40.00	10.00	3.00	0.50	7.19	5.78

	360.00	40.00	0.00	0.00	7.00	1.00	23.34	14.34

Table 6. Results of performance criteria for training, checking, testing, and all datasets of ANFIS models

	R2	MAPE	RMSE
ANFIS-I			
Training	0.9999	0.0022	0.0014
Checking	0.9789	21.4044	3.1580
Testing	0.9177	22.3580	6.4686
All data	0.9840	6.0797	2.6827
ANFIS-II			
Training	0.9999	0.0021	0.0007
Checking	0.9857	21.8939	2.9408
Testing	0.9336	22.5991	4.5766
All data	0.9911	6.2681	2.0416

Parametric study of ANFIS model

In order to investigate the effects of rubber addition along with other variables on compressive strength of the rubberized concrete obtained by ANFIS model, the output surfaces of the model were obtained which are presented in Fig. 14. In each plot, the effect of RB with one other variable on compressive strength is displayed in a 3D plot. As is seen from Fig. *(a), rubber increase up to 15% reduces the strength around 35% and cement content reduction increase the strength to some extent. In fig. 14(b), SF increase leads to strength increase and the lowest strength occurs 15% RB and 10% SF. The effect of Age, RH, and ZE are correspondingly depicted in Fig. 14 (c), (d), and (e) respectively.

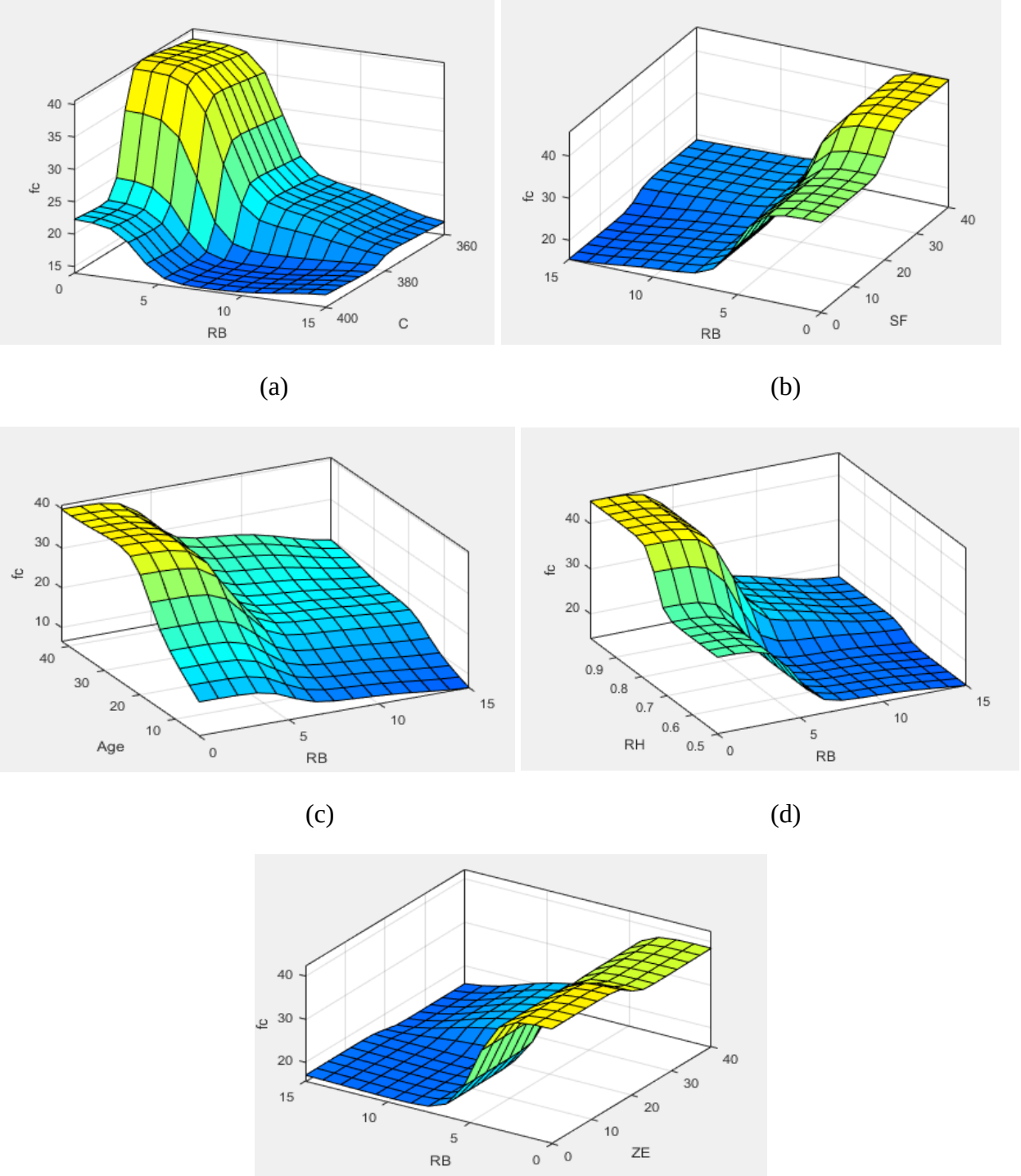

Fig. 14. Parametric study of the variables' effects on compressive strength of rubberized concrete from ANFIS model

7. Conclusion

In this study, experimental assessment and modeling of concrete containing scrap tire rubber was undertaken. Coarse aggregate was partially replaced by 10% and 15% of waste rubber and a fraction of cement was replaced by admixtures, namely silica fume and zeolite. The rubberized concrete samples were cured in two different conditions with RH of 1 and 0.5. several mixtures were cast and mechanical tests were carried out at different ages, namely 3, 7, 28 and 42 days to measure the compressive strength (f_c) and static elasticity modulus (E_s) of the rubberized concrete samples. Ultrasonic technique was employed to measure the primary and secondary wave velocities, and by measuring the density of concrete (ρ) mixtures and using the relationships, dynamic moduli of elasticity of concrete (E_d) were determined. In order to compare and validate the results obtained from ultrasonic technique, E_d was also calculated using ACI-318 equation based on the E_s and the correlation and errors were determined. It was found that the values of E_d estimated from ultrasonic technique were very close to those calculated from ACI equation, indicating the fact that ultrasonic can be employed as an accurate and easy method to estimate the mechanical properties of rubberized cement composite such as dynamic elasticity modulus. ANFIS modeling was also implemented to predict the f_c of rubberized concrete as a function of six influencing parameters such as C, SF, ZE, RB, RH, and age. Based on the performance criteria such as MAPE, RMSE, and R^2 calculated for ANFIS models, it was found that proposed ANFIS model can be used as a robust tool to predict the performance of complex composite such as rubberized concrete which are experimental and hard-to-model in nature.

References

[1] B.S. Thomas, R.C. Gupta, A comprehensive review on the applications of waste tire rubber in cement concrete, Renew Sustain Energy Rev, 54 (2016), pp. 1323-1333.

[2] ETRMA. ETRMA annual report 2013/2014, ETRMA. Brussels, Belgium; 2014.

[3] Rubber Manufacturers Association. US scrap tire management summary. Washington DC, USA; 2014.

[4] R. Siddique, T.R. Naik, Properties of concrete containing scrap-tire rubber - an overview, Waste Manage, 24 (6) (2004), pp. 563-569.

[5] M Jalal, A Pouladkhan, OF Harandi, D Jafari, "Comparative study on effects of Class F fly ash, nano silica and silica fume on properties of high performance self-compacting concrete" Construction and Building Materials, 2015; 94, 90-104.

[6] M Jalal, AA Ramezanianpour, MK Pool, Split tensile strength of binary blended self-compacting concrete containing low volume fly ash and TiO 2 nanoparticles, Composites Part B: Engineering, 2013; 55, 324-337.

[7] M Jalal, Corrosion resistant self-compacting concrete using micro and nano silica admixtures, Structural Engineering and Mechanics, 2014; 51 (3), 403-412.

[8] M Jalal, E Mansouri, Effects of fly ash and cement content on rheological, mechanical, and transport properties of high-performance self-compacting concrete, Science and Engineering of Composite Materials, 2012; 19(4): 393-405.

[9] M Jalal, E Mansouri, M Sharifipour, AR Pouladkhan, " Mechanical, rheological, durability and microstructural properties of high performance self-compacting concrete containing SiO 2 micro and nanoparticles", Materials & Design, 2012; 34: 389-400.

[10] R. Sharm, R.A.Khan, Sustainable use of copper slag in self-compacting concrete containing supplementary cementitious materials , Journal of Cleaner Production, 2018; 151: 179-192.

[11] N. Eldin, A. Senouci, Observations on rubberized concrete behavior, Cem Concr Aggregate, 15 (1) (1993), pp. 74-84.

[12] I.B. Topçu, The properties of rubberized concretes, Cem Concr Res, 25 (2) (1995), pp. 304-310

[13] Z. Li, F. Li, J.S.L. Li, Properties of concrete incorporating rubber tyre particles, Mag Concr Res, 50 (4) (1998), pp. 297-304

[14] L. Zheng, X.S. Huo, Y. Yuan, Experimental investigation on dynamic properties of rubberized concrete, Constr Build Mater, 22 (5) (2008), pp. 939-947

[15] F. Valadares, M. Bravo, J. de Brito, Concrete with used tire rubber aggregates: mechanical performance, ACI Mater J, 109 (3) (2012), pp. 283-292.

[16] M. Bravo, J. de Brito, Concrete made with used tyre aggregate: durability-related performance, J Cleaner Prod, 25 (2012), pp. 42-50.

[17] O. Youssf, M.A. ElGawady, J.E. Mills, X. MaAn, Experimental investigation of crumb rubber concrete confined by fibre reinforced polymer tubes, Constr Build Mater, 53 (2014), pp. 522-532

[18] A.P.C. Duarte, B.A. Silva, N. Silvestre, J. de Brito, E. Júlio, J.M. Castro, Experimental study on short rubberized concrete-filled steel tubes under cyclic loading, Compos Struct, 136 (2016), pp. 394-404

[19] A.P.C.Duarte, N.Silvestre, J.de Brito, E.Júlio, Numerical study of the compressive mechanical behaviour of rubberized concrete using the eXtended Finite Element Method (XFEM), Composite Structures, 179 (2017), 132-145

[20] M Jalal, R Moradi-Dastjerdi, M Bidram, Big data in nanocomposites: ONN approach and mesh-free method for functionally graded carbon nanotube-reinforced composites, Journal of Computational Design and Engineering, 2018, https://doi.org/10.1016/j.jcde.2018.05.003.

[21] Jodaei A, Jalal M, Yas MH, "Free vibration analysis of functionally graded annular plates by state-space based differential quadrature method and comparative modeling by ANN" Composites Part B: Engineering, 2012; 43 (2), 340-353.

[22] M Jalal, AK Mukhopadhyay, Z Grasley, Design, manufacturing, and structural optimization of a composite float using particle swarm optimization and genetic algorithm, Proceedings of the Institution of Mechanical Engineers, Part L: Journal of Materials: Design and Applications, DOI: 10.1177/1464420718755546.

[23] Jalal M, Ramezanianpour AA, "Strength enhancement modeling of concrete cylinders confined with CFRP composites using artificial neural networks". Composites Part B: Engineering, 2012; 43 (8), 2990-3000.

[24] Jalal M, Ramezanianpour AA, Pouladkhan AR, Tedro P, " Application of genetic programming (GP) and ANFIS for strength enhancement modeling of CFRP-retrofitted concrete cylinders", Neural Computing and Applications, 2013; 23(2): 455-470.

[25] Jalal M, "Soft computing techniques for compressive strength prediction of concrete cylinders strengthened by CFRP composites" Science and Engineering of Composite Materials, 2015; 22(1): 97-112.

[26] J.S.R. Jang, ANFIS: adaptive-network-based fuzzy inference system, IEEE Trans. Sys Man Cyber, 1993; 23 (3), 665-685.

[27] J.S.R. Jang, C.T. Sun, Nuro-fuzzy modeling and control, Proc IEEE, 1995; 83 (3).

[28] I.B. Topcu, M. Sarıdemir, Prediction of mechanical properties of recycled aggregate concretes containing silica fume using artificial neural networks and fuzzy logic Comput. Mater. Sci., 42 (1) (2008), pp. 74-82

[29] Bezdec, J.C., Pattern Recognition with Fuzzy Objective Function Algorithms, Plenum Press, New York, 1981.
[30] Chiu, S., “Fuzzy Model Identification Based on Cluster Estimation,” Journal of Intelligent & Fuzzy Systems, Vol. 2, No. 3, Sept. 1994.
[31] Z. Yuan LN. Wang, X. Ji, Prediction of concrete compressive strength: Research on hybrid models genetic based algorithms and ANFIS, Advances in Engineering Software, 2013;67: 156-163.